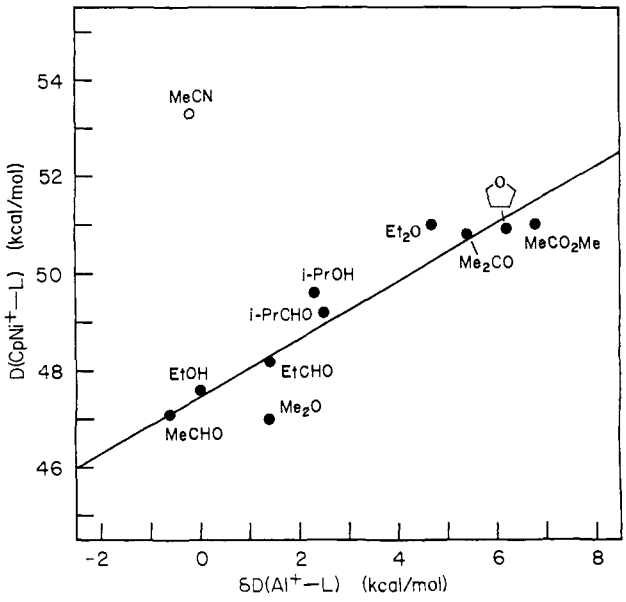

Figure 4. Comparison of relative ligand binding energies for $CpNi^+$ and Al^+. The solid line is a least-squares fit to the data: $\delta D(CpNi^+-L) = 0.595\delta D(Al^+-L) - 4.95$ kcal/mol (correlation coefficient = 0.93) omitting the data point for MeCN.

The data point for MeCN is clearly off the correlation line for the oxygen bases in Figure 4. The binding energy of MeCN to $CpNi^+$ is 6 kcal/mol stronger than expected from the correlation line for the measured value of $\delta D(Al^+-MeCN) = -0.2$ kcal/mol. Enhanced bonding of HCN, MeCN, and MeNC by about 6 kcal/mol to $CpNi^+$ compared to H^+ was noted by Corderman and Beauchamp and attributed to π back-bonding of Ni 3d electrons into empty π^* CN orbitals.[4]

The zero of the $\delta D(Al^+-L)$ scale is arbitrarily chosen because the present results do not allow an absolute calibration of the scale. The intercepts in Figures 3 and 4 are therefore not meaningful. Absolute lower limits for $D(Al^+-L)$ are available in some cases from the observation of certain elimination reactions.[6] The most useful of these is $D(Al^+-MeOH) \geq 38$ kcal/mol from the reaction of Al^+ with $MeCO_2Me$ to give $Al(MeOH)^+$ eliminating ketene.[6] This lower limit is the same as the $Li(MeOH)^+$ binding energy $D(Li^+-MeOH)^+ = 38$ kcal/mol showing that bonding to Al^+ is at least as strong as to Li^+, at least for alcohols and probably also for other oxygen bases. Better absolute calibration of the $\delta D(Al^+-L)$ scale awaits new results by other techniques.

The methods reported in the present work are generally applicable to determinations of relative ligand binding energies for other atomic metal cations. Results of studies of ligand binding energies to Mn^+ are described in a companion paper.[18] Studies are under way in our laboratory to measure relative ligand binding energies for complexes of Cu^+, Ni^+, Co^+, and $FeBr^+$ with two ligand molecules. The results of these studies along with the present work promise to significantly advance the quantitative understanding of metal-ligand bonding in the gas phase.

Acknowledgment is made to the National Science Foundation for support of this work by Grant CHE-76-17304.

Registry No. Ag^+, 14701-21-4; n-$PrCO_2Et$, 105-54-4; $EtCO_2Et$, 105-37-3; $MeCO_2Et$, 141-78-6; Et_2CO, 96-22-0; $EtCO_2Me$, 554-12-1; t-BuOMe, 1634-04-4; MeCOEt, 78-93-3; $MeCO_2Me$, 79-20-9; THF, 109-99-9; Me_2CO, 67-64-1; HCO_2n-Bu, 592-84-7; Et_2O, 60-29-7; HCO_2n-Pr, 110-74-7; C_6H_5CN, 100-47-0; HCO_2Et, 109-94-4; s-BuOH, 78-92-2; i-PrCHO, 78-84-2; n-PrCN, 109-74-0; i-BuOH, 78-83-1; i-PrOH, 67-63-0; n-BuOH, 71-36-3; HCO_2Me, 107-31-3; EtCN, 107-12-0; EtCHO, 123-38-6; Me_2O, 115-10-6; n-PrOH, 71-23-8; C_2H_3CN, 107-13-1; EtOH, 64-17-5; MeCN, 75-05-8; MeCHO, 75-07-0.

(18) Uppal, J. S.; Staley, R. H. *J. Am. Chem. Soc.*, following paper in this issue.

Relative Binding Energies of Organic Molecules to Mn^+ in the Gas Phase

Jack S. Uppal and Ralph H. Staley*[1]

Contribution from the Department of Chemistry, Massachusetts Institute of Technology, Cambridge, Massachusetts 02139. *Received May 6, 1981*

Abstract: Relative ligand binding energies, $\delta D(Mn^+-L)$, for Mn^+ with 33 organic molecules are determined. A pulsed laser volatilization/ionization source is used to generate Mn^+ which reacts with n-PrCl to give $Mn(n\text{-PrCl})^+$ in a two-step sequence. Addition of ligand molecules results in the production of $Mn(ligand)^+$ species as the predominant products. The equilibrium constant for the ligand-exchange reaction $MnL_1^+ + L_2 \rightleftarrows MnL_2^+ + L_1$ is measured to give relative free energies for ligand exchange. These are added and converted to enthalpies to give the $\delta D(Mn^+-L)$ scale with the assumption that entropy changes are small and can be neglected. The dependence of $\delta D(Mn^+-L)$ on functional group and substituent effects is analyzed. The results for Mn^+ are compared with available results for other reference acids: H^+, Al^+, Li^+, and $CpNi^+$. The slopes of linear correlations for oxygen bases in plots of relative ligand binding energies for one metal vs. those for another imply an order of effective metal-ligand bond distance of $H^+ < Al^+ < Mn^+ < Li^+$.

Gas-phase thermochemical data are useful in evaluating the energetics of reaction processes and in developing models of bonding. Ion cyclotron resonance (ICR) techniques have been used recently to obtain such data for various metal ion species.[2-11] In particular, relative bond dissociation energies, $D(M^+-L)$, the enthalpy of reaction 1, have been determined for complexes of

$$ML^+ \rightarrow M^+ + L \qquad \Delta H_1 = D(M^+-L) \qquad (1)$$

(1) Address correspondence to this author at Central Research Department, Experimental Station, DuPont Co. E356, Wilmington, Del. 19898.
(2) Staley, R. H.; Beauchamp, J. L. *J. Am. Chem. Soc.* **1975**, *97*, 5920.
(3) Woodin, R. L.; Beauchamp, J. L. *J. Am. Chem. Soc.* **1978**, *100*, 501.
(4) Corderman, R. R.; Beauchamp, J. L. *J. Am. Chem. Soc.* **1976**, *98*, 3998. Corderman, R. R.; Beauchamp, J. L. *J. Organomet. Chem.*, in press.

0002-7863/82/1504-1238$01.25/0

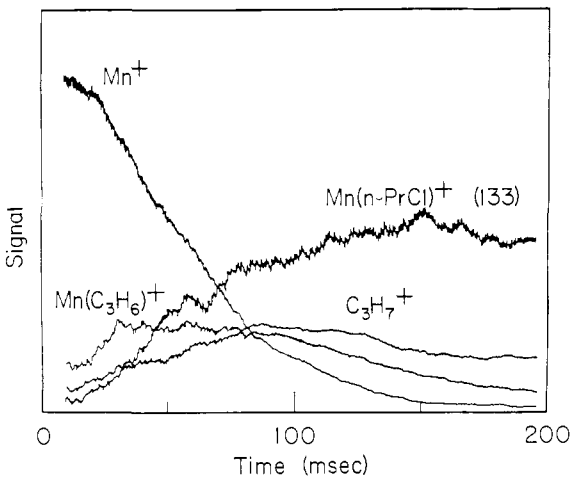

Figure 1. Variation of ion abundances with time following production of Mn^+ by the pulsed laser source in the presence of 2×10^{-6} Torr of *n*-PrCl. Mn^+ reacts with *n*-PrCl by chloride transfer (20%) to give $C_3H_7^+$ and by dehydrochlorination (80%) to give $Mn(C_3H_6)^+$. No $Mn(HCl)^+$ is observed. Propylene is readily displaced from $Mn(C_3H_6)^+$ by other molecules in the system giving $Mn(ligand)^+$ species; here, with only *n*-PrCl present, *n*-PrCl reacts to give $Mn(n\text{-PrCl})^+$ as the final product. The m/z value for the isotopic peak which was followed for the $Mn(n\text{-PrCl})^+$ species is given in parentheses.

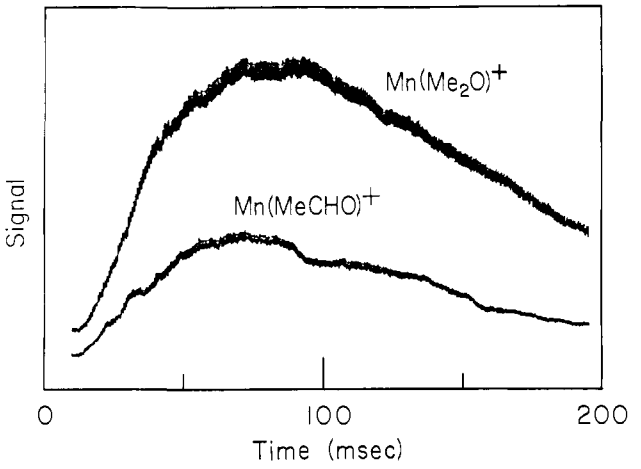

Figure 2. Variation of $Mn(Me_2O)^+$ and $Me(MeCHO)^+$ abundances with time for the Mn^+ source with a 3.06:1.00:0.68 mixture of Me_2O, MeCHO, and *n*-PrCl, respectively, at a total pressure of 14×10^{-6} Torr. Following initial reactions (not shown) the ratio of $Mn(Me_2O)^+$ and $Mn(MeCHO)^+$ abundances becomes constant as the reaction $Mn(Me_2O)^+ + MeCHO \rightleftarrows Mn(MeCHO)^+ + Me_2O$ approaches equilibrium. Double resonance experiments show that this ligand-exchange reaction is fast. The measured partial pressures of Me_2O and MeCHO and the ratio of ion abundances give an equilibrium constant of $K = 1.22$. The average of three determinations is $K = 1.28$ corresponding to a free-energy difference $\Delta G = -0.15$ kcal/mol. The slow decrease in total ion abundance in this figure results from ion loss by diffusion to the walls of the ICR cell.

Li^+,[2,3] $CpNi^+$ [4] ($Cp \equiv \eta^5\text{-}C_5H_5$), and Al^+ [5] by measuring equilibrium constants for ligand-exchange reaction 2. Our recent

$$ML_1^+ + L_2 \rightleftarrows ML_2^+ + L_1 \qquad (2)$$

$$\Delta H_2 = D(M^+\text{-}L_1) - D(M^+\text{-}L_2)$$

studies of Al^+ appear to provide an approach which will be generally applicable to determining $D(M^+\text{-}L)$ for a variety of metal cations.[5,6] In the present paper we report the first application of these techniques with a transition metal cation, Mn^+. The resulting scale of $D(Mn^+\text{-}L)$ is compared with $D(M^+\text{-}L)$ for Li^+, $CpNi^+$, Al^+, and H^+ to elucidate aspects of the bonding in these systems.

Experimental Section

The ICR instrumentation and techniques used in the present work have been previously described in detail.[5-9] The output of a pulsed YAG laser is focused onto a manganese target at the end of the ICR cell to produce atomic manganese cations. The initial mass spectrum shows only m/z 55, as expected. No peaks corresponding to Mn^{2+} or Mn_2^+ are observed. Chemicals were from commercial sources and were degassed by repeated freeze–pump–thaw cycles before use.

Pressure is measured with a Bayard–Alpert ionization gage located between the cell and the ion pump. Gas mixtures are prepared in the cell and partial pressures measured by difference as has been previously described.[5] Relative accuracy for the same gas of rate constants and product ratios is ±20% or better. Absolute accuracy for different gases is limited to a factor of 2 by the pressure measurements because the ion gage is not individually calibrated for each gas.

Results

Alkyl halides react with Mn^+ in a bimolecular sequence principally to produce a $Mn(ligand)^+$ species which can be used in ligand-exchange studies. Figure 1 shows the variation of ion abundances with time for Mn^+ in the presence of 2×10^{-6} Torr of *n*-PrCl. Mn^+ reacts with *n*-PrCl by chloride transfer, reaction 3, to give $C_3H_7^+$ and MnCl and by dehydrochlorination, reaction

$$Mn^+ + n\text{-PrCl} \xrightarrow{20\%} C_3H_7^+ + MnCl \qquad (3)$$

4, to give $Mn(C_3H_6)^+$ and HCl. No $Mn(HCl)^+$ is observed.

$$Mn^+ + n\text{-PrCl} \xrightarrow{80\%} Mn(C_3H_6)^+ + HCl \qquad (4)$$

Reactions 3 and 4 have a branching ratio of 1:4 with a total rate constant of 5×10^{-10} cm^3 molecule^{-1} s^{-1}. *n*-PrCl displaces propylene in $Mn(C_3H_6)^+$, reaction 5, to give $Mn(n\text{-PrCl})^+$. This

$$Mn(C_3H_6)^+ + n\text{-PrCl} \rightarrow Mn(n\text{-PrCl})^+ + C_3H_6 \qquad (5)$$

reacts slowly by chloride transfer, reaction 6, $k = 1 \times 10^{-10}$ cm^3 molecule^{-1} s^{-1}.

$$Mn(n\text{-PrCl})^+ + n\text{-PrCl} \rightarrow C_3H_7^+ + MnCl(n\text{-PrCl})^+ \qquad (6)$$

The ion chemistry of isopropyl chloride and isobutyl chloride with Mn^+ is similar to that of *n*-PrCl; chloride transfer and dehydrochlorination reactions are observed. Mn^+ is unreactive with many small organic molecules including EtCl, EtBr, MeOH, EtOH, Me_2O, Et_2O, MeCHO, MeCN, EtCN, and $MeNO_2$. $CHCl_3$ oxidizes Mn^+ to $MnCl^+$, reaction 7, which is followed by chloride transfer, reaction 8.

$$Mn^+ + CHCl_3 \rightarrow MnCl^+ + CHCl_2 \qquad (7)$$

$$MnCl^+ + CHCl_3 \rightarrow CHCl_2^+ + MnCl_2 \qquad (8)$$

In binary mixtures of *n*-PrCl with various organic molecules, L, propylene is displaced from $Mn(C_3H_6)^+$ by L, reaction 9. This

$$Mn(C_3H_6)^+ + L \rightarrow Mn(L)^+ + C_3H_6 \qquad (9)$$

results in a $Mn(L)^+$ species which does not react further with *n*-PrCl or L. Most molecules studied also displace *n*-PrCl from

(5) Uppal, J. S.; Staley, R. R. *J. Am. Chem. Soc.*, accompanying paper in this issue.
(6) Uppal, J. S.; Staley, R. H. *J. Am. Chem. Soc.*, preceding paper in this issue.
(7) Jones, R. W.; Staley, R. H. *J. Am. Chem. Soc.* **1980**, *102*, 3794. Uppal, J. S.; Staley, R. H. *Ibid.* **1980**, *102*, 4144.
(8) Kappes, M. M.; Staley, R. H. *J. Am. Chem. Soc.* **1981**, *103*, 1286. Kappes, M. M.; Staley, R. H. *J. Phys. Chem.* **1981**, *85*, 942–944.
(9) Kappes, M. M.; Jones, R. W.; Staley, R. H. *J. Am. Chem. Soc.* **1982**, *104*, 888.
(10) Stevens, A. E.; Beauchamp, J. L. *J. Am. Chem. Soc.* **1981**, *103*, 190.
(11) Freas, R. B.; Ridge, D. P. *J. Am. Chem. Soc.* **1980**, *102*, 7129. Allison, J.; Ridge, D. P. *Ibid.* **1979**, *101*, 4998. Dietz, T. G.; Chatellier, D. S.; Ridge, D. P. *Ibid.* **1978**, *100*, 4905. Allison, J.; Ridge, D. P. *Ibid.* **1976**, *98*, 7445; Allison, J., Ridge, D. P. *J. Organomet. Chem.* **1975**, *99*, C11.

Table I. Relative Gas-Phase Ligand Binding Energies to Mn^+ for Various Organic Molecules[a]

Ligand (L)	Measured $\Delta G_{exchange}$[b]	$\delta D(Mn^+-L)$[c]
MeCOEt		10.89
Me_3N	0.89	10.13
$MeCO_2Me$	0.13	10.00
Me_2CO	0.13	9.87
EtCN	0.06	9.81
THF[d]	0.75	9.18
Et_2O	0.02	9.16
HCO_2-n-Bu	0.01	9.15
t-BuOH	0.56	8.59
t-BuCHO	0.97	8.26
MeCN	0.12	8.19
HCO_2Et	0.05	8.14
i-PrCHO	0.83	7.31
n-PrCHO		7.20
t-BuOH	0.74	6.89
1,4-Dioxane[e]	0.32	6.21
EtCHO	0.63	6.57
HCO_2Me	0.05	6.47
n-PrOH	0.55	6.04
NH_3	0.09	5.69
Benzene[e]	1.14	5.02
MeCHO	1.23	5.24
Me_2O	0.80	5.09
EtOH	0.60	4.90
MeNCO	0.15	4.18
Oxirane	0.34	3.88
Me_2S	1.42	3.48
MeOH	0.56	3.32
n-PrSH	0.86	2.10
EtSH	0.16	1.43
HCN	1.22	1.12
H_2CO	0.67	0.88
MeSH	0.31	0.00
	0.56	
	1.27	
	1.04	

[a] All data in kcal/mol. [b] For the reaction $MnL_1^+ + L_2 \rightleftarrows MnL_2^+ + L_1$. [c] Values are relative to $D(Mn^+-MeSH) = 0$. Free-energy differences from the second column are added to give relative free energies which are converted to relative enthalpies, $\delta D(Mn^+-L)$, by assuming that entropy changes are small and can be neglected except for corrections for symmetry number changes. [d] Tetrahydrofuran. [e] In converting relative enthalpy a correction of $T\Delta S = 0.41$ kcal/mol is made for these compounds to correct for an assumed symmetry number decrease by a factor of 2 on formation of the Mn(ligand)$^+$ species.

$Mn(n\text{-PrCl})^+$, reaction 10. However, with $MeNO_2$ the reverse reaction is observed.

$$Mn(n\text{-PrCl})^+ + L \rightarrow Mn(L)^+ + n\text{-PrCl} \qquad (10)$$

In tertiary mixtures of *n*-PrCl with two molecules L_1 and L_2, reactions 9 and 10 result in the production of MnL_1 and MnL_2 species. Ligand exchange occurs by reaction 2; reaction 6 is suppressed. Although some of the initial Mn^+ abundance reacts to form $C_3H_7^+$ by reaction 3, the abundance of Mn(ligand)$^+$ species is sufficient to measure equilibrium constants for reaction 2 in favorable cases. Figure 2 shows the variation of ion abundances with time for a 3.1:1.0:0.7 mixture of Me_2O, MeCHO, and *n*-PrCl, respectively, at a total pressure of 1.4×10^{-5} Torr. The ratio of $Mn(Me_2O)^+$ to $Mn(MeCHO)^+$ abundances becomes constant after about 100 ms following the initial reactions. The ligand exchange reaction 2 for these ions with the Me_2O and MeCHO neutrals is shown by delayed ejection double resonance experiments to be rapid. An equilibrium constant for reaction 2 is calculated from the measured ratio of ion abundances and the partial pressures of the Me_2O and MeCHO neutrals. Three determinations give an average of $K = 1.28$ corresponding to a free-energy difference $-\Delta G_{exchange} = 0.15$ kcal/mol calculated from the relation $-\Delta G = RT \ln K$ for the operating temperature of 25 °C.

Scheme I

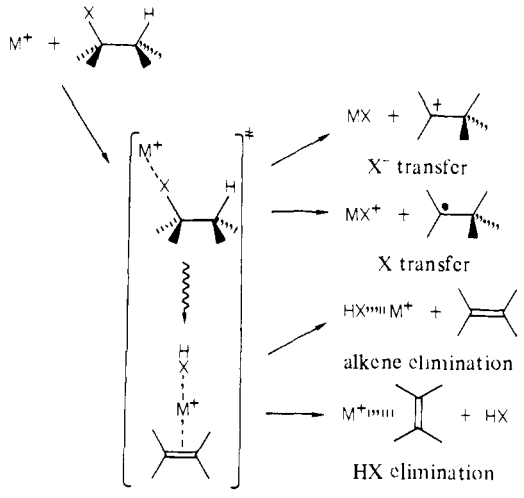

Equilibria were measured for reaction 2 for various pairwise combinations of 33 different molecules as ligands. Values for $\Delta G_{exchange}$ from these experiments are given in Table I. Each value represents an average of at least three determinations. The results are combined into a ladder to give a scale of relative free energies for ligand binding, $\delta\Delta G_{exchange}$, for each ligand. Redundant determinations in this scale provide an internal consistency check on the results. Agreement is found to within about ±0.2 kcal/mol.

Discussion

The observed ion chemistry of alkyl chlorides with Mn^+ is typical of that which has been observed with other atomic metal cations.[2,5,7,11,12] These transfer and dehydrochlorination reactions can be understood in terms of the mechanism of Scheme I. This type of mechanism was originally proposed to explain the chemistry of Li^+[2] and has since been found to occur in the chemistry of a number of other atomic metal cations[5,7,11] and NO^+[13] with alcohols, alkyl halides, and phenyl halides. Initial association of the metal cation, M^+, with the neutral reactant HYX leads to transfer of X or X^-, if exothermic, or internal rearrangement of the complex, elimination of HX from HYX, to give HX and Y bound separately to M^+. This dissociates to either $M(HX)^+$ and Y or $M(Y)^+$ and HX. Competition between X and X^- transfer is controlled by the relative ionization potentials of the dissociating species, that is, whether IP(MX) or IP(Y) is smaller. Competition between retention of HX and Y by M^+ is governed by the relative ligand–metal bond dissociation energies, that is, whether $D(M^+-HX)$ or $D(M^+-Y)$ is larger. For Mn^+ with *n*-PrCl both the chloride transfer and HCl elimination channels are active, reactions 3 and 4. When a single *n*-PrCl ligand has been added to Mn^+, i.e., for $M^+ = Mn(n\text{-PrCl})^+$, the chloride transfer channel is still active, reaction 6, but the elimination channel is not. For Mn^+ with $CHCl_3$ the chlorine transfer channel is active, reaction 7. With the product of this reaction, $MnCl^+$, chloride transfer is preferred, reaction 8. Together, reactions 7 and 8 indicate that $IP(MnCl) < IP(CHCl_2) < IP(MnCl_2)$.

Observations of the transfer reactions 3, 6, 7, and 8 establish lower limits on bond energies for some manganese–chlorine species.

(12) Hodges, R. V.; Armentrout, P. B.; Beauchamp, J. L. *Int. J. Mass Spectrom. Ion Phys.* **1979**, *29*, 375–390.
(13) Williamson, A. D.; Beauchamp, J. L. *J. Am. Chem. Soc.* **1975**, *97*, 5714.

The chloride transfer reactions 3, 6, and 8 establish the limits $D(Mn^+-Cl^-) > D(n\text{-}Pr^+-Cl^-) = 167$ kcal/mol,[14] $D(Mn(n\text{-}PrCl)^+-Cl^-) > 167$ kcal/mol,[14] and $D(MnCl^+-Cl^-) > D(CHCl_2^+-Cl^-) = 180$ kcal/mol.[14] The chlorine transfer reaction 7 implies $D(Mn^+-Cl) > D(CHCl_2-Cl)$; a reliable value for $D(CHCl_2-Cl)$ is not available from the literature, however. These values are all in ranges typical of values observed for other transition metals.[7]

The dehydrochlorination of *n*-PrCl by Mn^+, reaction 4, provides a convenient bimolecular route to preparation of $Mn(ligand)^+$ complexes for ligand-exchange studies with Mn^+. This reaction has the desirable characteristics that it is fast, stops after one ligand is bound to Mn^+, and gives a product with a relatively weakly bound ligand. Competition by reaction 3 is a negative factor since 20% of the initial Mn^+ is lost to this channel. The 80% remaining was easily adequate for the ligand-exchange studies, however. The $Mn(C_3H_6)^+$ product of reaction 4 is readily displaced by the molecules studied as ligands in this work to give $Mn(ligand)^+$ complexes. A similar role to that played by reaction 4 in this study was played by dehydrochlorination of *i*-PrCl by Li+ and by dehydration of EtOH by Al^+ in ligand-exchange studies with Li^+ and Al^+, respectively.[2,5,6] Suitable reagents to be used in this capacity can likely be found for other atomic metal cations allowing ligand-exchange studies to be undertaken. It thus appears that this approach along with the pulsed laser volatilization/ionization source may be generally applicable for such studies.

Ligand Binding Energies. Relative enthalpies of binding to Mn^+, $\delta D(Mn^+-L)$, for the 33 molecules studied are given in Table I. These are given relative to $D(Mn^+-MeSH) = 0$ which is chosen arbitrarily. The absolute zero of this enthalpy scale cannot be determined from the present work. The enthalpy scale is obtained from the free-energy scale by the assumption that entropy changes are small and tend to cancel so that they may be neglected except for corrections for symmetry changes.[15]

The symmetry correction to ΔS is necessary when the symmetry number of the $Mn(ligand)^+$ complex is different from that of the ligand. This is clearly the case for benzene and 1,4-dioxane where the symmetry numbers are reduced by a factor of 2 on formation of the $Mn(ligand)^+$ species. The relative free energies are therefore increased by $T\Delta S = -RT \ln 2 = -0.41$ kcal/mol in calculating the relative enthalpies, $\delta D(Mn^+-L)$, Table I, for benzene and 1,4-dioxane. For the other molecules studied as ligands in this work, it is assumed that the symmetry numbers of the ligand and $Mn(ligand)^+$ species are the same.[16]

Changes in moments of inertia could also make a significant contribution to ΔS for reaction 2. This contribution has been analyzed in detail for $Li(ligand)^+$ complexes by Woodin and Beauchamp.[3] Accurate treatment of this contribution requires knowledge of the geometries of the species involved. Geometries are not available for the $Mn(ligand)^+$ species. However, this effect seems likely to be unimportant in the present work. Moment of inertia changes are important when manganese–ligand bonding distance and ligand mass are significantly different for the two ligands. The ligands studied are similar in mass and can be expected to bond similarly to Mn^+. Neglect of entropy changes, except for the symmetry number correction, thus appears to be an acceptable assumption in the present work.

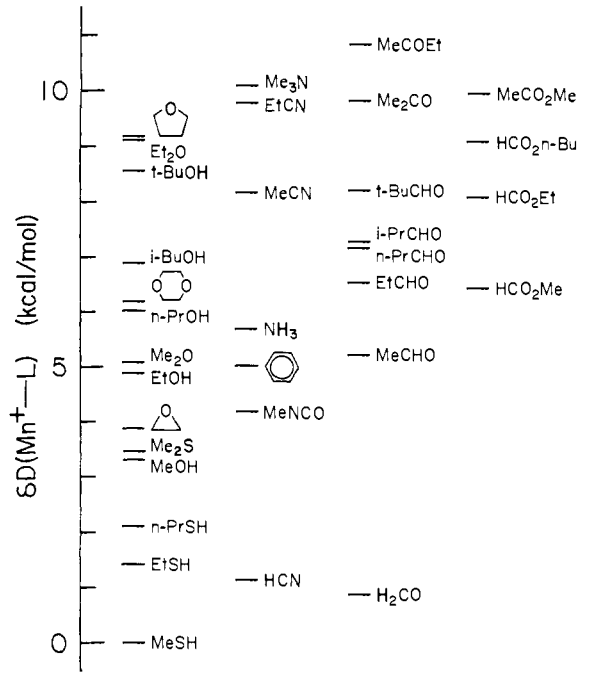

Figure 3. Binding energies of 33 molecules to Mn^+, arranged by functional group, relative to $D(Mn^+-MeSH) = 0$.

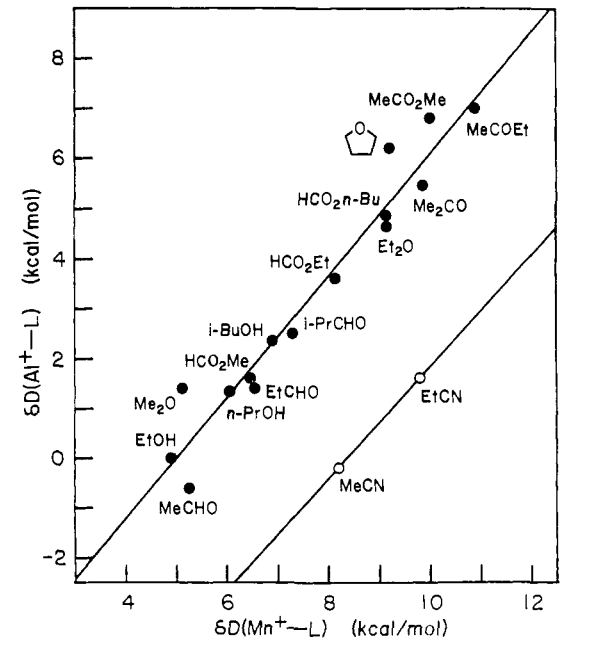

Figure 4. Comparison of relative binding energies of molecules to Al^+ and Mn^+. The upper solid line is a least-squares fit to the data for the oxygen bases: $\delta D(Al^+-L) = 1.22\delta D(Mn^+-L) - 6.1$ kcal/mol (correlation coefficient $r = 0.97$). The line through the two data points for nitriles is given by $\delta D(Al^+-L) = 1.13\delta D(Mn^+-L) - 9.4$ kcal/mol. This corresponds to an offset on the $\delta D(Mn^+-L)$ axis of 3.4 kcal/mol.

Relative binding energies for the 33 molecules studied in this work, arranged by functional group, are plotted in Figure 3. Within each functional group series, substitution of a larger alkyl group for a smaller one is seen to lead to a systematic increase in $\delta D(Mn^+-L)$. Similar systematic alkyl substituent effects have been observed for proton affinities,[17] $PA(B) = D(B-H^+)$, and for ligand binding energies to Li^+ [2] and Al^+ [6].

(14) Calculated using $\Delta H_{f0}(n\text{-PrCl}) = -31.0 \pm 0.2$ kcal/mol and $\Delta H_{f0}(CHCl_3) = -24.6 \pm 0.2$ kcal/mol from Cox, J. D.; Pilcher, G. "Thermochemistry of Organic and Organometallic Compounds"; Academic Press: New York, 1970. $\Delta H_{f0}(i\text{-}C_3H_6^+) = 101$ kcal/mol and $\Delta H_{f0}(Cl^-) = -54.6$ kcal/mol from Rosenstock, H. M.; Draxl, K.; Steiner, B. W.; Herron, J. T. *J. Phys. Chem. Ref. Data, Suppl. 1* **1977**, *6*; and $\Delta H_{f0}(CHCl_2^+) = 211.2 \pm 0.4$ kcal/mol from Werner, A. S.; Tsai, B. P.; Baer, T. *J. Chem. Phys.* **1974**, *60*, 3650; and Lossing, F. P. *Bull. Soc. Chim. Belg.* **1972**, *81*, 125. It is assumed that the $[Mn(n\text{-PrCl})^+]^*$ intermediate in reaction 3 rearranges releasing the energy of rearrangement to the $i\text{-}C_3H_7^+$ and MnCl products before dissociating. This gives a lower lower limit than if a $n\text{-}C_3H_7^+$ product is assumed. See ref 5. A similar assumption is made for reaction 6.

(15) Benson, S. W. "Thermochemical Kinetics", 2nd ed.; Wiley-Interscience: New York, **1976**; p 76.

(16) The $Mn(ligand)^+$ species for Me_2CO, THF, Et_2O, Me_2O, ethylene oxide, Me_2S, and H_2CO are assumed to have a planar structure with a twofold symmetry axis like the neutrals. While bent structures for these ions cannot be ruled out, theoretical calculations for the $Li(H_2O)^+$ species have shown the symmetric planar geometry to be the most stable: Clementi, E.; Popkie, H. *J. Chem. Phys.* **1972**, *57*, 1077.

(17) Wolf, J. F.; Staley, R. H.; Koppel, I.; Taagepera, M.; McIver, R. T., Jr.; Beauchamp, J. L.; Taft, R. W. *J. Am. Chem. Soc.* **1977**, *99*, 5417.

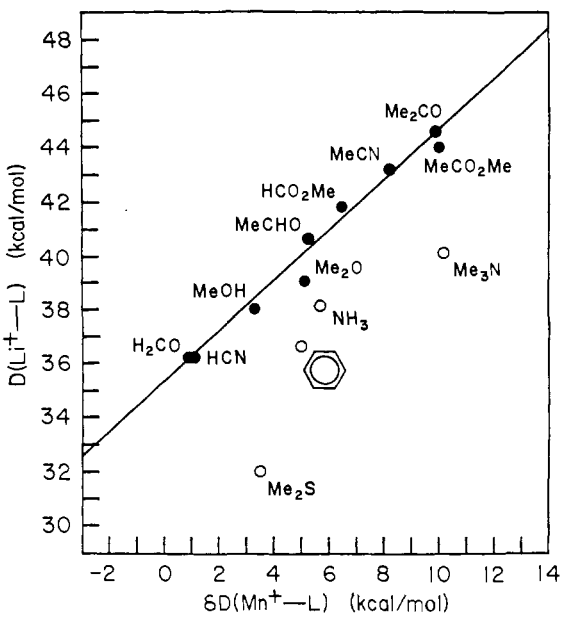

Figure 5. Comparison of relative binding energies of molecules to Li^+ and Mn^+. The solid line is a least-squares fit to the data for the seven oxygen bases and two nitriles (solid circles): $D(Li^+–L) = 0.93\delta D(Mn^+–L) + 35.3$ kcal/mol ($r = 0.98$).

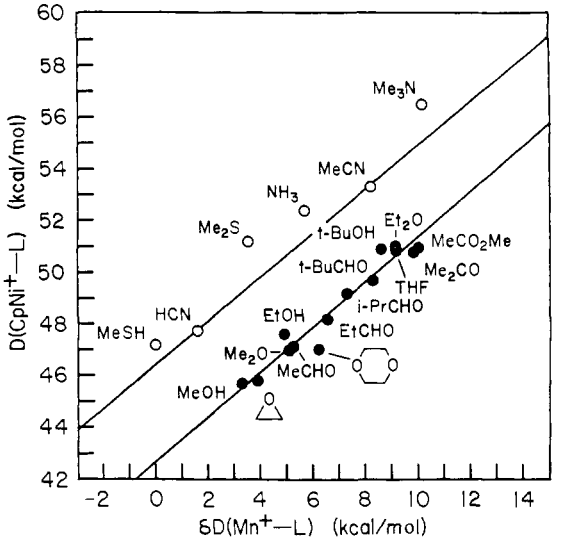

Figure 6. Comparison of relative binding energies of molecules to $CpNi^+$ and Mn^+. The solid line is a least-squares fit to the data for the oxygen bases (solid circles): $D(CpNi^+–L) = 0.87\delta D(Mn^+–L) + 42.6$ kcal/mol ($r = 0.97$). The line defined by the points for the two nitriles is given by $D(CpNi^+–L) = 0.79\delta D(Mn^+–L) + 46.8$ kcal/mol corresponding to an offset on the $D(CpNi^+–L)$ axis of 3.7 kcal/mol.

The bonding interaction of Mn^+ with ligand molecules should be largely ionic in character. Mn^+ has a ^7S ground state corresponding to an $[Ar](3d)^5(4s)^1$ configuration.[18] Excitation to one of the next higher states, $[Ar](3d)^5(4s)^1\ ^5S$ at 1.2 eV or $[Ar](3d)^6\ ^5D$ at 1.8 eV, should be unimportant for ligand bonding. In bonding to ground-state Mn^+, ligands are attracted by interaction of intrinsic and induced ligand dipoles with the charge on Mn^+. Some covalent bonding can occur by delocalization of electrons from occupied ligand orbitals into the empty 4p or half-filled 4s and 3d orbitals on Mn^+. This delocalization will be limited by repulsion by the electrons in the half-filled 4s and 3d orbitals. Some covalent bonding can also occur by delocalization of 3d electrons on Mn^+ into unoccupied ligand π^* orbitals, π back-bonding. This can occur only for certain ligand molecules where suitable orbitals are available.

Comparison of the ligand binding energy results for Mn^+ with available results for other reference acids reveals some interesting points about the nature of the metal–ligand bonding interaction. Figure 4 shows a plot of the relative ligand binding energies to Al^+, $\delta D(Al^+–L)$, vs. the results for Mn^+, $\delta D(Mn^+–L)$. The 15 oxygen bases show a good linear correlation. A least-squares fit to these data gives: $\delta D(Al^+–L) = 1.22\delta D(Mn^+–L) - 6.1$ kcal/mol (correlation coefficient $r = 0.97$). The oxygen bases include alkyl alcohols, ethers, aldehydes, ketones, and esters. These all fall approximately on the same line. The slope of this line, 1.22, shows that as basicitiy increases the strength of the bond to Al^+ increases slightly faster than that to Mn^+. This suggests that the ligand–metal bond distance for $Al(ligand)^+$ complexes is slightly shorter than for $Mn(ligand)^+$ complexes. With a shorter bond distance the effect of a larger alkyl substituent may be expected to be greater since it is closer to the charge center which remains on the metal atom.

Two data points for nitriles in Figure 4 fall on a line given by $\delta D(Al^+–L) = 1.13\delta D(Mn^+–L) - 9.4$ kcal/mol. This has about the same slope as the line for oxygen bases but is offset by 3.4 kcal/mol on the $\delta D(Mn^+–L)$ axis. The offset can be attributed to π back-bonding by 3d electrons on Mn^+ into empty π^* CN orbitals on the nitriles. Offsets of 6 kcal/mol for nitriles compared to oxygen bases have been observed in plots of binding energies to $CpNi^+$ vs. binding energies to H^+ [4] and to Al^+ [6]. The smaller effect by about a half which is observed for Mn^+ compared to $CpNi^+$ is reasonable for π back-bonding since the 3d orbitals on Mn^+ have only one electron each whereas for $CpNi^+$ they are nearly full.

Comparison of the resuults for Mn^+ with data for Li^+,[2] Figure 5, also shows a good linear correlation for oxygen bases. Remarkably, the two nitriles in this data set are on the line with the oxygen bases. A least-squares fit to the seven oxygen bases and two nitriles gives $D(Li^+–L) = 0.93\delta D(Mn^+–L) + 35.3$ kcal/mol ($r = 0.98$). Here the slope shows slightly stronger binding to Mn^+ compared to Li^+ with increasing basicity suggesting that the metal–ligand bond distance for Mn^+ is slightly shorter than for Li^+.

Several bases fall off the linear correlation in Figure 5: Me_2S (7.0), benzene (3.6), NH_3 (2.7), and Me_3N (5.0), where the offset on the $\delta D(Mn^+–L)$ axis from the linear correlation is given for each molecule in parentheses in kilocalories/mole. The offsets toward stronger bonding to Mn^+ for Me_2S and benzene could be explained in terms of π back-bonding which certainly does not occur for Li^+ but could be of some importance for Mn^+ as suggested by the preceding discussion of the Al^+ vs. Mn^+ comparison in Figure 4. However, the lack of offset for the nitriles in Figure 5 must then be regarded as bizarre since an offset is seen for the nitriles in the Al^+ vs. Mn^+ comparison of Figure 4.

It is therefore reasonable to conclude that other factors in addition to π back-bonding and of comparable magnitude contribute to determining the offsets for functional group correlation lines. Such factors might include the strength of the ionic bond, bond distance, and covalent σ bonding.

In a given correlation plot of binding energies of molecules to one metal vs. those to another, it is thus to be expected that the molecules for each functional group may in general fall on different lines. Some of these lines may happen to be approximately the same such as alcohols and esters in Figure 4 and nitriles and the oxygen bases in Figure 5. Some evidence for this view has been previously noted. In the comparison of $D(B–H^+)$ with $\delta D(Al^+–L)$ it was seen that esters fall on a line somewhat apart from the general correlation line for all bases.[6] The correlations plotted in Figure 6 for $CpNi^+$ vs. Mn^+ data and Figure 7 for H^+ [17,19] vs. Mn^+ data lend further support to this idea. In Figure 6 oxygen bases including alcohols, ethers, aldehydes, ketones, and esters fall approximetely on a single line: $D(CpNi^+–L) = 0.87\delta D(Mn^+–L) + 42.6$ kcal/mol ($r = 0.97$). Two nitriles define a line

(18) Moore, C. E. "Atomic Energy Levels", NBS Circular 467, U.S. Government Printing Office: Washington, D.C., 1952; Vol. 2.

(19) Aue, D. H.; Bowers, M. T. In "Gas Phase Ion Chemistry"; Bowers, M. T., Ed.; Academic Press: New York, 1979; Vol. 2, Chapter 9.

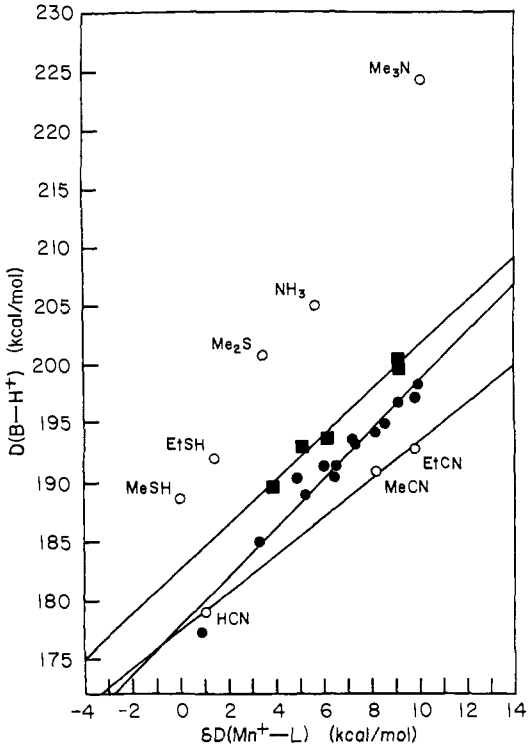

Figure 7. Comparison of proton affinities, $D(B-H^+)$, to ligand binding energies to Mn^+ for 27 molecules. Least-squares fit lines are drawn for three nitriles, $D(B-H^+) = 1.63\delta D(Mn^+-L) + 177.2$ kcal/mol ($r = 0.999$); five ethers (solid squares), $D(B-H^+) = 1.90\delta D(Mn^+-L) + 182.5$ kcal/mol ($r = 0.99$), and other oxygen bases (solid circles), $D(B-H^+) = 2.08\delta D(Mn^+-L) + 177.6$ kcal/mol ($r = 0.98$).

of similar slope but offset by 3.7 kcal/mol on the $D(CpNi^+-L)$ axis: $D(CpNi^+-L) = 0.79\delta D(Mn^+-L) + 46.8$. Sulfur bases (MeSH and Me_2S) and amines (NH_3 and Me_3N) are also offset, falling somewhat beyond the line for the nitriles. In the H^+ vs. Mn^+ plot, Figure 7, ethers clearly fall on a separate line: $D(B-H^+) = 1.90\delta D(Mn^+-L) + 182.5$ kcal/mol ($r = 0.99$), from the line for the other oxygen bases: $D(B-H^+) = 2.08\delta D(Mn^+-L) + 177.6$ kcal/mol ($r = 0.98$). A separate line is also seen for nitriles: $D(B-H^+) = 1.63\delta D(Mn^+-L) + 177.2$ kcal/mol ($r = 0.999$). Significant variation of both offsets and slopes is found among these lines.

The variation of slopes of the linear correlations in the comparisons studied to date follow a systematic pattern. The slopes of the lines for oxygen bases for H^+, Al^+, Li^+, and $CpNi^+$ vs. Mn^+ are 2.08, 1.22, 0.93, and 0.87, respectively, Figures 4–7. For nitriles these slopes are 1.63, 1.30, 0.93, and 0.79 in the same order. Slopes for all the linear correlations obtained to date are given in Table II. The results all follow the same order: $H^+ < Al^+ < Mn^+ < Li^+ < CpNi^+$. As previously noted[6] and discussed above, this order may reflect the ligand–metal bonding distance for the atomic metal cations, H^+ having the shortest effective bonding distance and Li^+ the longest. Where there is significant delocalization of charge away from the metal, as with H^+, the distance to the charge center rather than the bond distance to the center

Table II. Slopes for Linear Correlations in Plots of Ligand Binding Energies to One Metal vs. Another for Oxygen Bases[a]

metal cation	versus H^+	Al^+	Mn^+	Li^+	$CpNi^+$
H^+	1.00	1.53	2.08	2.71	3.38
Al^+	0.65	1.00	1.22		1.68
Mn^+	0.48	0.82	1.00	1.08	1.15
Li^+	0.37		0.93	1.00	
$CpNi^+$	0.30	0.60	0.87		1.00

[a] The slopes are from correlation plots given in the present work, Figures 4–7, reference 6 (H^+ vs. Al^+ and $CpNi^+$ vs. Al^+), reference 2 (H^+ vs. Li^+), and reference 4 (H^+ vs. $CpNi^+$).

of the metal atom may be the controlling parameter. For $CpNi^+$ it seems likely that the slope of the correlation plot is due to another factor, the presence of a second ligand. Polarization of the $CpNi^+$ group produces an internal dipole moment which opposes the dipole moment induced in the ligand in the CpNi(ligand)$^+$ complex. This tends to cancel the favorable interaction of $CpNi^+$ charge with the induced ligand dipole. No such cancellation occurs for the atomic metal cation complexes with ligands since the atomic metal cations do not have internal dipole moments.

In conclusion, the results for ligand binding energies to Mn^+ and their comparison to the data sets for H^+, Al^+, Li^+, and $CpNi^+$ show linear variation of basicity with alkyl substitution for a given functional group. The slope of this effect appears to depend on a parameter for each reference acid which may be related to effective metal–ligand bond distance. Variation of both the slope and offset of these lines among functional groups is also observed. Understanding of the dependence on functional groups would benefit from absolute calibration of the relative ligand binding energy scales obtained in the present work. Such calibration awaits results by other techniques since the present work gives only relative ligand binding energies. The present relative ligand binding energy results do afford significant new insights into the nature of the metal–ligand bonding interaction for the simple case of an atomic metal cation interacting with a single ligand in the gas phase. These quantitative thermochemical results should benefit development of more exact theoretical models of metal–ligand interactions. The methods used in the present work are generally applicable to determinations of relative ligand binding energies for other atomic metal cations. Studies have recently been completed in our laboratory determining relative ligand binding energies for complexes of Cu^+, Ni^+, Co^+, and $FeBr^+$ with two ligands and will be reported shortly. An account of one aspect of these results has been submitted.[9]

Acknowledgement is made to the National Science Foundation for support of this work by Grant CHE-76-17304.

Registry No. Mn^+, 14127-69-6; MeCOEt, 78-93-3; Me_3N, 75-50-3; $MeCO_2Me$, 79-20-9; Me_2CO, 67-64-1; EtCN, 107-12-0; THF, 109-99-9; Et_2O, 60-29-7; HCO_2-*n*-Bu, 592-84-7; *t*-BuOH, 75-65-0; *t*-BuCHO, 630-19-3; MeCN, 75-05-8; HCO_2Et, 109-94-4; *i*-PrCHO, 78-84-2; *n*-PrCHO, 123-72-8; *i*-BuOH, 78-83-1; 1,4-dioxane, 123-91-1; EtCHO, 123-38-6; HCO_2Me, 107-31-3; *n*-PrOH, 71-23-8; NH_3, 7664-41-7; benzene, 71-43-2; MeCHO, 75-07-0; Me_2O, 115-10-6; EtOH, 64-17-5; MeNCO, 624-83-9; oxirane, 75-21-8; Me_2S, 75-18-3; MeOH, 67-56-1; *n*-PrSH, 107-03-9; EtSH, 75-08-1; HCN, 74-90-8; H_2CO, 50-00-0; MeSH, 74-93-1.